

Fast isogeometric solvers for hyperbolic wave propagation problems

M. Łoś,⁽¹⁾ P. Behnoudfar⁽²⁾, M. Paszyński⁽¹⁾, V. M. Calo^(2,3,4)

⁽¹⁾ *Department of Computer Science, Faculty of Computer Science, Electronics and Telecommunications, AGH University of Science and Technology, Krakow, Poland*

e-mail: paszynsk@agh.edu.pl

e-mail: marcin.los.91@gmail.com

⁽²⁾ *Applied Geology Department,
Western Australian School of Mines,*

Faculty of Science and Engineering, Curtin University, Perth, WA, Australia,

e-mail: victor.calo@curtin.edu.au

⁽³⁾ *Mineral Resources, Commonwealth Scientific and Industrial Research Organisation (CSIRO),
Kensington, WA, Australia 6152*

⁽⁴⁾ *Curtin Institute for Computation, Curtin University, Perth, WA, Australia 6845*

Abstract

We use the alternating direction method to simulate implicit dynamics. Our spatial discretization uses isogeometric analysis. Namely, we simulate a (hyperbolic) wave propagation problem in which we use tensor-product B-splines in space and an implicit time marching method to fully discretize the problem. We approximate our discrete operator as a Kronecker product of one-dimensional mass and stiffness matrices. As a result of this algebraic transformation, we can factorize the resulting system of equations in linear (i.e., $O(N)$) time at each step of the implicit method. We demonstrate the performance of our method in the model P-wave propagation problem. We then extend it to simulate the linear elasticity problem once we decouple the vector problem using alternating triangular methods. We prove theoretically and experimentally the unconditional stability of both methods.

Keywords: isogeometric analysis, implicit dynamics, wave propagation problems, linear computational cost, direct solvers

1. Introduction

The alternating directions method (ADS) introduced in [30, 12, 32, 5] to deal with finite difference simulations for time-dependent problems. The method currently solves a broad class of problems [19, 20].

Isogeometric analysis (IGA) [9], uses B-splines or NURBS [31] basis functions in finite element simulations. IGA has multiple applications in time-dependent simulations, including phase field models [10, 11], phase-separation simulations with application to cancer growth simulations [17, 18], wind turbine aerodynamics [24], incompressible hyper-elasticity [13], turbulent flow simulations [7], transport of drugs in cardiovascular applications [23] as well as the blood flow simulations and drug transport in arteries simulations [3, 2, 6].

Recently, Gao et al. [14, 15, 16] applied the direction splitting method to the rapid solution of explicit dynamics using isogeometric analysis on tensor-product grids. These direction splitting schemes deliver a fast inversion method for the spatial discretization by grouping one-dimensional B-splines along particular spatial axes. For similar methods for fast simulations of explicit dynamics refer to [25, 33, 26, 27, 21, 35].

In this paper, we extend this methodology to hyperbolic scalar problems by collecting different terms as a sequence of multi-banded inversions. Then, we extend these ideas to hyperbolic vector problems, where the model problem is isotropic linear elasticity. First, its corresponding differential operator is decoupled (for more details, see [42]), and then our idea is employed. Finally, we prove the unconditional stability of the schemes as well as their order of convergence.

The structure of the paper is the following. In section 2, we start from the description of the direction splitting for the P-wave equation. Next, in Section 3, we show the stability analysis for the P-wave problem. Section 4 presents the numerical results for the three-dimensional P-wave propagation problem. In Section 5, we extend our method to elastic wave propagation, stability analysis in Section 6, and provide numerical evidence in Section 7. In Section 8, we analyze the order of the schemes. We describe our conclusions in Section 9.

2. Direction splitting for scalar P-wave equation

We describe the methodology by directly applying it to a model problem. We first solve the scalar P-wave equation problem given by

$$\ddot{u} - \Delta u = f, \tag{1}$$

where the over dot represents a time derivative, and Δ is the Laplacian operator. We discretize time as follows

$$\ddot{u}_{n+1} - \Delta u_{n+1} = f_{n+1} \quad (2)$$

and use a Newmark expansion from time step n to $n + 1$ [28]

$$u_{n+1} = u_n + \tau \dot{u}_n + \frac{1}{4}\tau^2 \ddot{u}_{n+1} \quad (3)$$

so that

$$\ddot{u}_{n+1} - \frac{1}{4}\tau^2 \Delta \ddot{u}_{n+1} = \Delta u_n + \tau \Delta \dot{u}_n + f_{n+1} \quad (4)$$

We treat u_n , \dot{u}_n and \ddot{u}_n as three independent variables. Thus, we can update \dot{u}_n according to

$$\dot{u}_{n+1} = \dot{u}_n + \frac{1}{2}\tau \ddot{u}_{n+1} \quad (5)$$

As for the u_n , we use a backward Taylor expansion to obtain

$$u_n = u_{n+1} - \tau \dot{u}_{n+1} + \frac{1}{2}\tau^2 \ddot{u}_{n+1} \quad (6)$$

and so

$$u_{n+1} = u_n + \tau \dot{u}_{n+1} - \frac{1}{2}\tau^2 \ddot{u}_{n+1} \quad (7)$$

The full scheme is thus the following:

$$\left\{ \begin{array}{l} \ddot{u}_{n+1} - \frac{1}{4}\tau^2 \Delta \ddot{u}_{n+1} = \Delta u_n + \tau \Delta \dot{u}_n + f_{n+1} \\ \dot{u}_{n+1} = \dot{u}_n + \frac{1}{2}\tau \ddot{u}_{n+1} \\ u_{n+1} = u_n + \tau \dot{u}_{n+1} - \frac{1}{2}\tau^2 \ddot{u}_{n+1} \end{array} \right. \quad (8)$$

We can compute u_{n+1} and \dot{u}_{n+1} given \ddot{u}_{n+1} .

For the first equation, we test with function w . Thus, the full scheme becomes

$$(w, \ddot{u}_{n+1}) + \frac{1}{4}\tau^2 (\nabla w, \nabla \ddot{u}_{n+1}) = (w, \Delta u_n + \tau \Delta \dot{u}_n + f_{n+1}). \quad (9)$$

We discretize

$$w = \sum_{ab} n_a m_b C_{ab} \quad \ddot{u}_{n+1} = \sum_{cd} n_c m_d D_{cd} \quad (10)$$

where $n_a m_b$ and $n_c m_d$ denotes the tensor-product of one-dimensional B-spline, which form a two-dimensional basis function, and C_{ab} and D_{cd} denotes the coefficients associated with the degrees of freedom. The left-hand side of the equation is

$$(n_a m_b C_{ab}, n_c m_d D_{cd}) + \frac{1}{4} \tau^2 (n'_a m_b C_{ab}, n'_c m_d D_{cd}) + \frac{1}{4} \tau^2 (n_a m'_b C_{ab}, n_c m'_d D_{cd}).$$

Assuming that the geometry of the domain is simple, we can express the mapping as a separable function. Thus, we can now split the left-hand side of the system as follows

$$(n_a m_b, n_c m_d) C_{ab} D_{cd} + (n'_a, n'_c)_x \frac{1}{4} \tau^2 (m_b, m_d)_y C_{ab} D_{cd} + (m'_b, m'_d)_x \frac{1}{4} \tau^2 (n'_a, n'_c)_y C_{ab} D_{cd}.$$

We define the following one-dimensional mass and stiffness matrices

$$\begin{aligned} (n_a, n_c)_x &= M_x, \\ (n_b, n_d)_y &= M_y, \\ (n'_a, n'_c)_x &= K_x, \\ (n'_b, n'_d)_y &= K_y, \end{aligned} \tag{11}$$

and rewrite the entire system as

$$\begin{aligned} \left(M_x \otimes M_y + \frac{1}{4} \tau^2 (M_x \otimes K_y + K_x \otimes M_y) \right) \ddot{U}^{n+1} &= -(M_x \otimes K_y + K_x \otimes M_y) U^n \\ &\quad - \tau (M_x \otimes K_y + K_x \otimes M_y) \dot{U}^n + F^{n+1} \end{aligned} \tag{12}$$

We can now approximate the system as

$$\begin{aligned} (M_x + \frac{1}{4} \tau^2 K_x) \otimes (M_y + \frac{1}{4} \tau^2 K_y) &= M_x \otimes M_y \\ &\quad + \frac{1}{4} \tau^2 M_x \otimes K_y + \frac{1}{4} \tau^2 K_x \otimes M_y + \frac{1}{16} \tau^4 K_x \otimes K_y \\ &\approx M_x \otimes M_y + \frac{1}{4} \tau^2 (M_x \otimes K_y + K_x \otimes M_y). \end{aligned}$$

Dropping the red term results in the following

$$\begin{aligned} (M_x + \frac{\tau^2}{4} K_x) \otimes (M_y + \frac{\tau^2}{4} K_y) \ddot{U}_{n+1} &= -(M_x \otimes K_y + K_x \otimes M_y) (U^n + \tau \dot{U}^n) + F_{n+1} \\ \dot{U}_{n+1} &= \dot{U}_n + \frac{1}{2} \tau \ddot{U}_{n+1} \\ U_{n+1} &= U_n + \tau \dot{U}_{n+1} - \frac{1}{2} \tau^2 \ddot{U}_{n+1}. \end{aligned} \tag{13}$$

3. Spectral analysis of splitting for wave-propagation problem

In this section, we analyze the stability of the splitting scheme to show it is unconditionally stable. The analysis follows closely the approach introduced in [45, 38, 47]. Throughout this section, we set $F = 0$.

3.1. Stability of the splitting scheme

We consider the spectral decomposition of each of the directional matrices K_ξ with respect to its directional M_ξ (see for example [44]) and obtain

$$K_\xi = M_\xi P_\xi D_\xi P_\xi^{-1}, \quad (14)$$

where D_ξ is a diagonal matrix containing the eigenvalues of the generalized eigenvalue problem

$$K_\xi v_\xi = \lambda_\xi M_\xi v_\xi \quad (15)$$

and the columns of P_ξ are the eigenvectors of the generalized problem. Herein, $\xi = x, y, z$ specifies each of the coordinate directions. We state the analysis for 2D splitting and calculate the required terms given by (for details see [45, 48])

$$\begin{aligned} \tilde{G}^{-1} &= P_x E_x P_x^{-1} M_x^{-1} \otimes P_y E_y P_y^{-1} M_y^{-1}, \\ \tilde{G}^{-1} M &= (P_x \otimes P_y) \cdot (E_x \otimes E_y) \cdot (P_x^{-1} \otimes P_y^{-1}), \\ \tilde{G}^{-1} K &= (P_x \otimes P_y) \cdot (E_x D_x \otimes E_y + E_x \otimes E_y D_y) \cdot (P_x^{-1} \otimes P_y^{-1}). \end{aligned} \quad (16)$$

where $G = M + \eta K$ with $\eta = \frac{\tau^2}{4}$, and

$$E_\xi = (I + \eta D_\xi)^{-1}, \quad \xi = x, y. \quad (17)$$

If we use the following identity:

$$I = P_x I_x P_x^{-1} \otimes P_y I_y P_y^{-1} = (P_x \otimes P_y) \cdot (I_x \otimes I_y) \cdot (P_x^{-1} \otimes P_y^{-1}), \quad (18)$$

then, the blocks of the amplification matrix are

$$\begin{aligned}
\Xi_{11} &= (P_x \otimes P_y) \cdot (I_x \otimes I_y - \tau^2 (E_x D_x \otimes E_y + E_x \otimes E_y D_y)) \cdot (P_x^{-1} \otimes P_y^{-1}), \\
\Xi_{12} &= (P_x \otimes P_y) \cdot (I_x \otimes I_y - \tau^2 (E_x D_x \otimes E_y + E_x \otimes E_y D_y)) \cdot (P_x^{-1} \otimes P_y^{-1}), \\
\Xi_{13} &= (P_x \otimes P_y) \cdot \left(-\frac{1}{2} (I_x \otimes I_y) + ((I_x \otimes I_y) - E - \right. \\
&\quad \left. \frac{\tau^2}{2} (E_x D_x \otimes E_y + E_x \otimes E_y D_y)) \right) \cdot (P_x^{-1} \otimes P_y^{-1}), \\
\Xi_{21} &= (P_x \otimes P_y) \cdot \left(-\tau^2 \frac{1}{2} (E_x D_x \otimes E_y + E_x \otimes E_y D_y) \right) \cdot (P_x^{-1} \otimes P_y^{-1}), \\
\Xi_{22} &= (P_x \otimes P_y) \cdot \left(I_x \otimes I_y - \tau^2 \frac{1}{2} (E_x D_x \otimes E_y + E_x \otimes E_y D_y) \right) \cdot (P_x^{-1} \otimes P_y^{-1}), \\
\Xi_{23} &= (P_x \otimes P_y) \cdot \left(\left(I_x \otimes I_y - \frac{1}{2} (E_x \otimes E_y) - \frac{\tau^2}{4} (E_x D_x \otimes E_y + E_x \otimes E_y D_y) \right) \right) \cdot (P_x^{-1} \otimes P_y^{-1}), \\
\Xi_{31} &= (P_x \otimes P_y) \cdot (-\tau^2 (E_x D_x \otimes E_y + E_x \otimes E_y D_y)) \cdot (P_x^{-1} \otimes P_y^{-1}), \\
\Xi_{32} &= (P_x \otimes P_y) \cdot (-\tau^2 (E_x D_x \otimes E_y + E_x \otimes E_y D_y)) \cdot (P_x^{-1} \otimes P_y^{-1}), \\
\Xi_{33} &= (P_x \otimes P_y) \cdot \left(I_x \otimes I_y - (E_x \otimes E_y) - \frac{\tau^2}{2} (E_x D_x \otimes E_y + E_x \otimes E_y D_y) \right) \cdot (P_x^{-1} \otimes P_y^{-1}).
\end{aligned} \tag{19}$$

By denoting $\zeta = E_x D_x \otimes E_y + E_x \otimes E_y D_y$ and $\tilde{E} = E_x \otimes E_y$, we write the matrix as:

$$\begin{aligned}
\Xi &= \begin{bmatrix} P_x \otimes P_y & \mathbf{0} & \mathbf{0} \\ \mathbf{0} & P_x \otimes P_y & \mathbf{0} \\ \mathbf{0} & \mathbf{0} & P_x \otimes P_y \end{bmatrix} \begin{bmatrix} I - \tau^2 \zeta & I - \tau^2 \zeta & \frac{1}{2} I + \left(-\tilde{E} - \frac{\tau^2}{2} \zeta \right) \\ -\frac{1}{2} \tau^2 \zeta & I - \frac{1}{2} \tau^2 \zeta & I - \frac{1}{2} \tilde{E} - \frac{\tau^2}{4} \zeta \\ -\tau^2 \zeta & -\tau^2 \zeta & I - \tilde{E} - \frac{\tau^2}{2} \zeta \end{bmatrix}^n \\
&\quad \begin{bmatrix} P_x^{-1} \otimes P_y^{-1} & \mathbf{0} & \mathbf{0} \\ \mathbf{0} & P_x^{-1} \otimes P_y^{-1} & \mathbf{0} \\ \mathbf{0} & \mathbf{0} & P_x^{-1} \otimes P_y^{-1} \end{bmatrix}.
\end{aligned} \tag{20}$$

To prove the unconditional stability of the method, we calculate its spectral radius:

$$\tilde{\Xi} = \begin{bmatrix} I - \tau^2 \zeta & I - \tau^2 \zeta & \frac{1}{2} I + \left(-\tilde{E} - \frac{\tau^2}{2} \zeta \right) \\ -\frac{1}{2} \tau^2 \zeta & I - \frac{1}{2} \tau^2 \zeta & I - \frac{1}{2} \tilde{E} - \frac{\tau^2}{4} \zeta \\ -\tau^2 \zeta & -\tau^2 \zeta & I - \tilde{E} - \frac{\tau^2}{2} \zeta \end{bmatrix} \tag{21}$$

First, by defining $\sigma = \tau^2 D_\xi$, we consider the two limiting cases for σ : $\sigma \rightarrow 0$ and $\sigma \rightarrow \infty$. In the limit $\sigma \rightarrow 0$, since D_ξ is diagonal, $E_\xi \rightarrow I$ and consequently, we

have $\tau^2\zeta \rightarrow 0$ and $E \rightarrow I$. Hence, $\tilde{\Xi}$ becomes upper triangular with the following eigenvalues:

$$\lambda_1 = \lambda_2 = 1, \quad \lambda_3 = 0. \quad (22)$$

Hence, due to the equal multiplicity with the dimension of the stiffness matrix in 2D, K , the eigenvalues are bounded by 1, and the method is unconditionally stable. In the case of the infinite time-step size, the matrix $\tilde{\Xi}$ becomes:

$$\tilde{\Xi} = \begin{bmatrix} I & I & \frac{1}{2}I \\ \mathbf{0} & I & I \\ \mathbf{0} & \mathbf{0} & I \end{bmatrix}. \quad (23)$$

Therefore, in the limit $\sigma \rightarrow \infty$, we obtain the eigenvalues $\lambda = 1$. This analysis shows that the method is stable but not A-stable. Additionally, one can show that the scheme is stable for any finite time step size.

Remark 1. *The study of the unconditional stability of 3D splitting follows the same logic, but it is more involved.*

4. Numerical results for scalar P-wave equation

We test our algorithm in a scalar P-wave propagation problem over a three-dimensional mesh with $32 \times 32 \times 32$ elements and time step size $dt = 0.01$. We plot in Figures 1 and 3 the kinetic, potential, and total energies through the entire simulation, as well as some snapshots from intermediate time steps.

We also verify numerically second order in time of the method, as presented in Figure 2.

5. Direction splitting for elastic wave propagation

In this section, we solve the linear elasticity problem given by

$$\begin{cases} \rho \partial_{tt} \mathbf{u} = \nabla \cdot \boldsymbol{\sigma} + \mathbf{F} & \text{on } \Omega \times [0, T] \\ \mathbf{u}(x, 0) = u_0 & \text{for } x \in \Omega \\ \boldsymbol{\sigma} \cdot \hat{\mathbf{n}} = 0 & \text{on } \partial \Omega \end{cases} \quad (24)$$

where $\Omega = [0, 1]^3$ is a unit cube, \mathbf{u} is a three-dimensional displacement vector to be calculated, ρ is material density, \mathbf{F} is the applied external force, and $\boldsymbol{\sigma}$ is the Cauchy stress tensor, given by

$$\sigma_{ij} = c_{ijkl} \epsilon_{lk}, \quad \epsilon_{ij} = \frac{1}{2} (\partial_j u_i + \partial_i u_j) \quad (25)$$

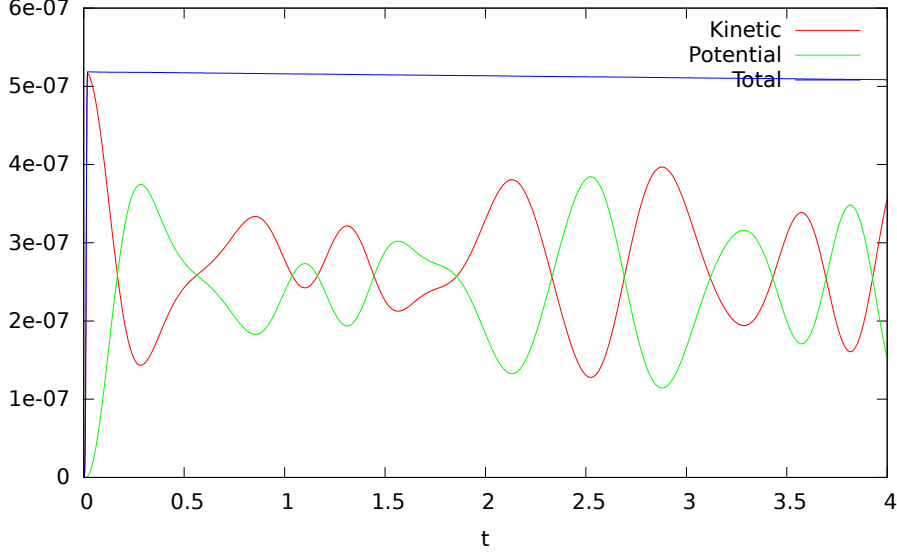


Figure 1: The kinetic, potential and total energy through the entire simulation of P-wave propagation with time step 0.01.

and \mathbf{c} is the elasticity tensor. Corresponding semi-discretized weak formulation is given by

$$(\ddot{u}_i^{n+1}, w) = \frac{1}{\rho} (\sigma_{ij,j} + F_i, w), \quad (26)$$

where for repeated indexes we apply the Einstein summation convention, and

$$\sigma_{ij} = 2\mu\epsilon_{ij} + \lambda\epsilon_{kk}\delta_{ij}, \quad (27)$$

by denoting $\epsilon_{ij} = \frac{1}{2}(\partial_j u_i + \partial_i u_j)$. The weak form is obtained by taking the scalar product with a test functions w_i and integrating by parts

$$\rho(w_i, \ddot{u}_i^{n+1}) + (w_{(i,j)}, \sigma_{ij}) = (F_i, w), \quad (28)$$

where

$$w_{(i,j)} = \frac{w_{i,j} + w_{j,i}}{2}. \quad (29)$$

We discretize

$$w_i = \sum_{ab} n_a m_b C_{ab}^i \quad \ddot{u}_i^{n+1} = \sum_{cd} n_c m_d D_{cd}^i \quad (30)$$

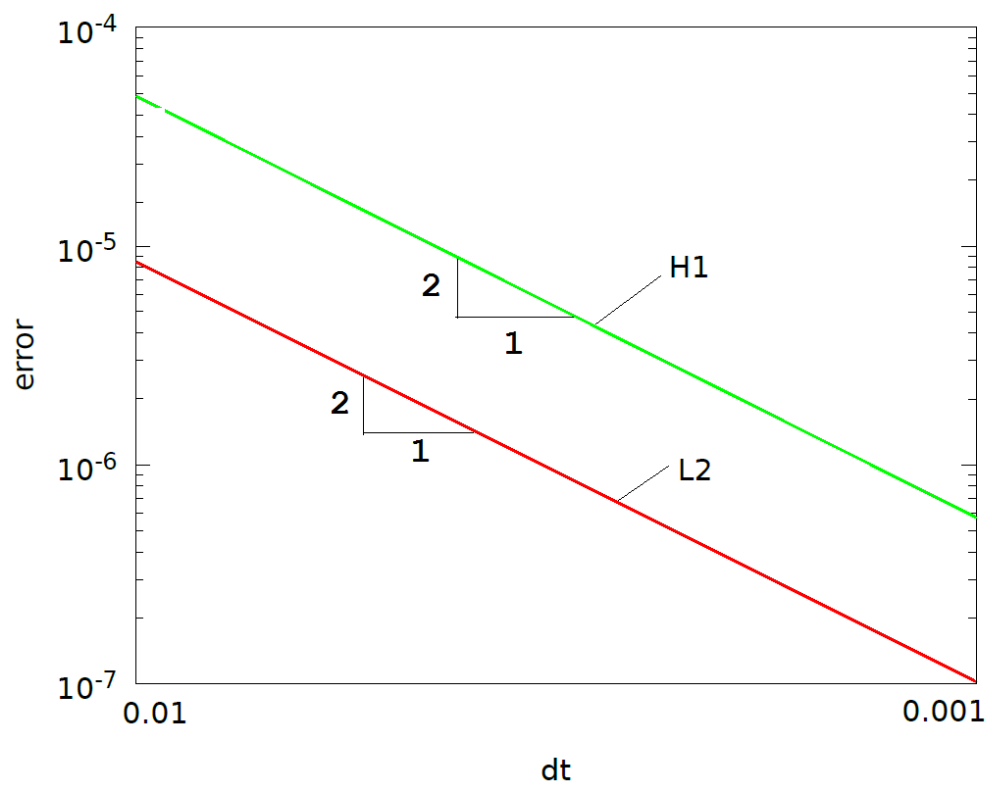


Figure 2: The second order time integration scheme for P-wave equation.

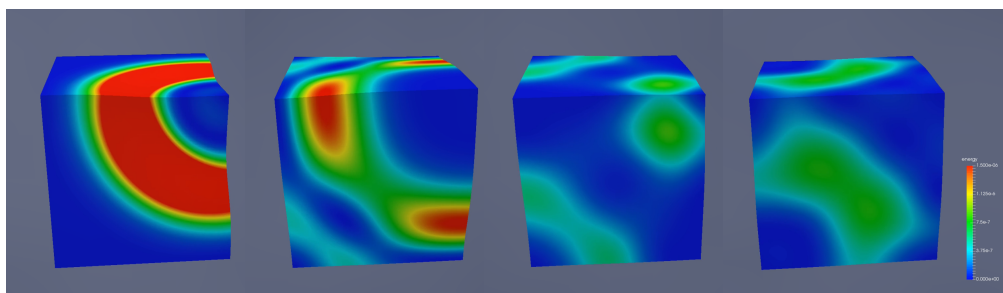


Figure 3: Stable simulation.

where $n_a m_b$ and $n_c m_d$ denotes the tensor product two-dimensional B-spline basis functions, and $C_{ab}^i, i = 1, 2$ and D_{cd}^i denotes the coefficients. We can obtain

$$w_{1,1} = n'_a m_b C_{ab}^1 \quad (31)$$

$$w_{1,2} = n_a m'_b C_{ab}^1 \quad (32)$$

$$w_{2,1} = n'_a m_b C_{ab}^2 \quad (33)$$

$$w_{2,2} = n_a m'_b C_{ab}^2 \quad (34)$$

Thus,

$$\begin{aligned} w_{(1,1)} &= \frac{w_{1,1} + w_{1,1}}{2} = w_{1,1} = n'_a m_b C_{ab}^1, \\ w_{(1,2)} &= \frac{w_{1,2} + w_{2,1}}{2} = \frac{n_a m'_b C_{ab}^1 + n'_a m_b C_{ab}^2}{2}, \\ w_{(2,1)} &= \frac{w_{2,1} + w_{1,2}}{2} = w_{(1,2)} = \frac{n_a m'_b C_{ab}^1 + n'_a m_b C_{ab}^2}{2}, \\ w_{(2,2)} &= \frac{w_{2,2} + w_{2,2}}{2} = w_{2,2} = n_a m'_b C_{ab}^2. \end{aligned} \quad (35)$$

Moreover,

$$2w_{(1,2)} = n_a m'_b C_{ab}^1 + n'_a m_b C_{ab}^2. \quad (36)$$

We substitute the constitutive law into the weak form

$$(w_{(i,j)}, \sigma_{ij}) = 2\mu(w_{(i,j)}, \epsilon_{ij}) + \lambda(w_{(i,j)}, \epsilon_{kk}\sigma_{ij}). \quad (37)$$

Since $u_{(i,j)} = \epsilon_{ij}$ and $u_{k,k} = u_{(k,k)} = \epsilon_{kk}$, we utilize the definition of the Kronecker delta

$$(w_{(i,j)}, \sigma_{ij}) = 2\mu(w_{(i,j)}, u_{(i,j)}) + \lambda(w_{(j,j)}, u_{(k,k)}). \quad (38)$$

Let us rewrite the differential operator Υ that corresponds the linear-elasticity problem in 2D as

$$\Upsilon = \begin{bmatrix} \Upsilon_{11} & \Upsilon_{12} \\ \Upsilon_{21} & \Upsilon_{22} \end{bmatrix}, \quad (39)$$

where

$$\begin{aligned} \Upsilon_{11} &= (2\mu + \lambda)K_x \otimes M_y + \mu K_x \otimes M_y, \\ \Upsilon_{12} &= \mu B_x \otimes B_y^T + \lambda B_x^T \otimes B_y, \\ \Upsilon_{21} &= \mu B_x^T \otimes B_y + \lambda B_x \otimes B_y^T, \\ \Upsilon_{22} &= \mu K_x \otimes M_y + (2\mu + \lambda)K_x \otimes M_y, \end{aligned} \quad (40)$$

and we also denote the mixed matrices as

$$\begin{aligned}
(n'_a, n_c)_x &= B_x, \\
(n_a, n'_c)_x &= B_x^T, \\
(n'_b, n_d)_y &= B_y, \\
(n_b, n'_d)_y &= B_y^T.
\end{aligned} \tag{41}$$

Next, we use the idea of alternating triangular methods [42] to the first-order evolutionary equations to construct an alternative to the second-order equations where to apply our scheme [41]. The alternating triangular method allows us to extend the operator splitting given by

$$\Upsilon = \Upsilon^{(1)} + \Upsilon^{(2)}, \tag{42}$$

where, taking into account (39), we define

$$\Upsilon^{(1)} = \begin{bmatrix} \frac{1}{2}\Upsilon_{11} & \mathbf{0} \\ \Upsilon_{21} & \frac{1}{2}\Upsilon_{22} \end{bmatrix}, \quad \Upsilon^{(2)} = \begin{bmatrix} \frac{1}{2}\Upsilon_{11} & \Upsilon_{12} \\ \mathbf{0} & \frac{1}{2}\Upsilon_{22} \end{bmatrix}. \tag{43}$$

Finally, we solve the fully discrete problem using a two-stage approach. The predictor stage calculates $\tilde{U}^{n+1} = [\tilde{U}_x^{n+1}, \tilde{U}_y^{n+1}]^T$ as

$$\rho M_x \otimes M_y \left(\frac{\tilde{U}^{n+1} - 2U^n + U^{n-1}}{\tau^2} \right) + \Upsilon^{(1)} \left(\frac{\tilde{U}^{n+1} + U^{n-1}}{2} \right) + \Upsilon^{(2)} U^n = f^n. \tag{44}$$

To enhance the solution, we solve the following corrector stage

$$\rho M_x \otimes M_y \left(\frac{U^{n+1} - 2U^n + U^{n-1}}{\tau^2} \right) + \Upsilon^{(1)} \left(\frac{\tilde{U}^{n+1} + U^{n-1}}{2} \right) + \Upsilon^{(2)} \left(\frac{U^{n+1} + U^{n-1}}{2} \right) = f^n. \tag{45}$$

Following the approach of (44) and (45), one can solve two uncoupled problems to find \tilde{U}_x^{n+1} and then \tilde{U}_y^{n+1} . Next, the corrected solution U_y^{n+1} is obtained and is employed to find U_x^{n+1} . To adapt the idea of splitting, we collect the terms and

approximate the operators applied on the unknown vectors $\tilde{U}_x^{n+1}, \tilde{U}_y^{n+1}$ as

$$\begin{aligned}
& \left[M_x \otimes M_y + \frac{\tau^2}{4\rho} ((2\mu + \lambda)K_x \otimes M_y + \mu K_x \otimes M_y) \right] \tilde{U}_x^{n+1} \simeq \\
& \quad \left(M_x + \frac{\tau^2}{4\rho} (2\mu + \lambda)K_x \right) \otimes \left(M_y + \frac{\tau^2}{4\rho} \mu K_y \right) \tilde{U}_x^{n+1}, \\
& \left[M_x \otimes M_y + \frac{\tau^2}{4\rho} (\mu K_x \otimes M_y + (2\mu + \lambda)K_x \otimes M_y) \right] \tilde{U}_y^{n+1} \simeq \\
& \quad \left(M_x + \frac{\tau^2}{4\rho} \mu K_x \right) \otimes \left(M_y + \frac{\tau^2}{4\rho} (2\mu + \lambda)K_y \right) \tilde{U}_y^{n+1}.
\end{aligned} \tag{46}$$

The splitting of the operators in the corrector stage follows the same argument as (46). Considering the splitting method, we approximate $M + \frac{\tau^2}{4} \Upsilon^{(1)}$ and $M + \frac{\tau^2}{4} \Upsilon^{(2)}$ using $M + \frac{\tau^2}{4} \tilde{\Upsilon}^{(1)}$ and $M + \frac{\tau^2}{4} \tilde{\Upsilon}^{(2)}$, respectively, by ignoring the higher order terms $\mathcal{O}(\tau^4)$.

5.1. Stability of the method

In this section, we study the stability of the resulting scheme (44)-(46) by rewriting the generalized form as

$$D \frac{U^{n+1} - 2U^n + U^{n-1}}{\tau^2} + \Upsilon U^n = f^n, \quad n = 1, 2, \dots, N, \tag{47}$$

Taking into account the decomposition (44), (45) and the splitting (46), we denote D as $D = \left(\rho M + \sigma \tau^2 \tilde{\Upsilon}^{(1)} \right) \frac{1}{\rho M} \left(\rho M + \sigma \tau^2 \tilde{\Upsilon}^{(2)} \right)$. Hence, we have

$$\rho M + \sigma \tau^2 \Upsilon \leq D. \tag{48}$$

Here, we employ the argument proposed in [?] to study the stability as follows.

Theorem 1. *For the method described in (44)-(46), the a priori estimate for $\sigma \geq 0.25$ holds,*

$$\|U^{n+1}\|_* \leq \|U^n\|_* + \tau \|f^n\|, \tag{49}$$

where

$$\|U^{n+1}\|_*^2 = \left\| \frac{U^{n+1} - U^n}{\tau} \right\|_D^2 + \left\| \frac{U^{n+1} + U^n}{2} \right\|_{\Upsilon}^2. \tag{50}$$

Proof. To prove, we closely follow the proof in [41] by doing the inner product of (47) by $(U^{n+1} - 2U^n + U^{n-1})$. We obtain

$$\begin{aligned} & \left\| \frac{U^{n+1} - U^n}{\tau} \right\|_D^2 - \left\| \frac{U^n - U^{n-1}}{\tau} \right\|_D^2 + \left\| \frac{U^{n+1} + U^n}{2} \right\|_\Upsilon^2 - \left\| \frac{U^n + U^{n-1}}{2} \right\|_\Upsilon^2 \\ &= (f^n, U^{n+1} - 2U^n + U^{n-1}) \end{aligned} \quad (51)$$

The left-hand side of the (51) becomes

$$(\|U^{n+1}\|_* + \|U^n\|_*) (\|U^{n+1}\|_* - \|U^n\|_*) \quad (52)$$

On the right-hand side of (51), we have

$$\begin{aligned} \left(f^n, \frac{U^{n+1} - 2U^n + U^{n-1}}{\tau} \right) &\leq \left\| \frac{U^n - U^{n-1}}{\tau} \right\| \left(\left\| \frac{U^n - U^{n-1}}{\tau} \right\| + \left\| \frac{U^{n+1} - U^n}{\tau} \right\| \right) \\ &\leq \|f^n\| (\|U^{n+1}\|_* + \|U^n\|_*) \end{aligned} \quad (53)$$

Hence, we obtain an *a priori* estimate for the method that establishes its stability with respect to the initial data and the right-hand side. This completes the proof. \square

Remark 2. *Again, for the sake of brevity, we omit the proof for 3D problems, which follows the same logic.*

6. Numerical results for linear elasticity

We apply our algorithm to a linear elasticity problem in 3D with a mesh composed of 32^3 elements with a time-step size 10^{-2} . We plot the evolution of the kinetic, potential, and total energies through the entire simulation. We also provide snapshots from intermediate time steps, see Figures 4 and 6. We verify numerically that the method has second-order accuracy in time of the method, see Figure 5.

7. Conclusions

In this paper, we introduce a space-time discretization using the alternating direction method to simulate hyperbolic problems. In particular, we use high-order, smooth isogeometric basis functions in space and an implicit time marching scheme in time. We build the spatial discretization on tensor-product spaces. We then use the Kronecker-product structure of the algebraic system to invert a sequence of implicit time steps with a cost proportional to the total number of degrees of freedom in the

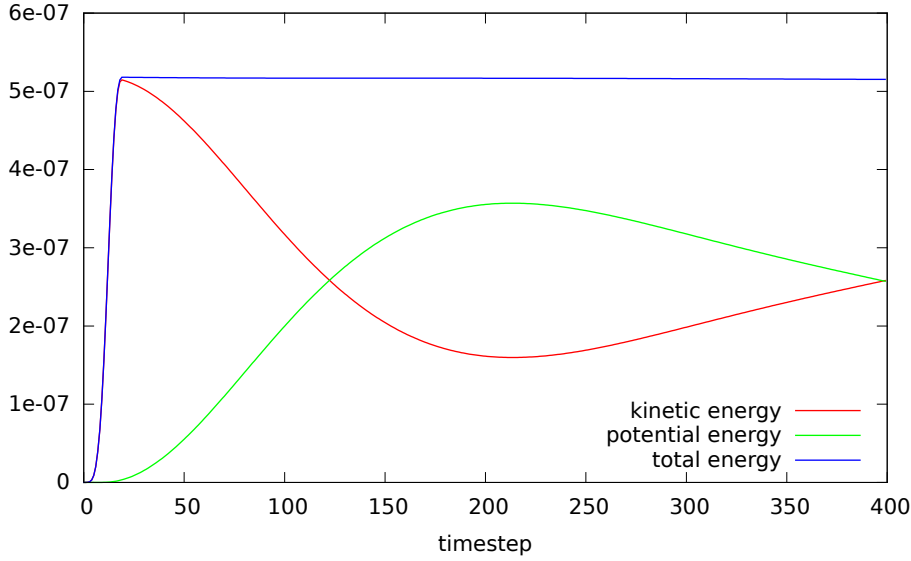


Figure 4: The kinetic, potential, and total energies for the entire simulation, time-step size 10^{-2} . The total energy remains constant.

system. We analyze the stability of the hyperbolic solvers theoretically and, then, verify the results numerically. Namely, we show the unconditional stability of the methods and verify the second-order accuracy of the time scheme experimentally. We show the performance for 2D and 3D for the scalar and vectorial differential systems. Future work will involve development of splitting schemes for Maxwell equations [49] and performing parallel version of the code [50].

Acknowledgments

National Science Centre, Poland, partially funded the work of Maciej Paszyński, Marcin Łoś, and the visit of Pouria Behnoudfar to Kraków via the grants 2017/26/M/ST1/00281 and 2015/ 19/B/ST8/01064. This publication was also made possible in part by the CSIRO Professorial Chair in Computational Geoscience at Curtin University and the Deep Earth Imaging Enterprise Future Science Platforms of the Commonwealth Scientific Industrial Research Organisation, CSIRO, of Australia. The European Union’s Horizon 2020 Research and Innovation Program of the Marie Skłodowska-Curie grant agreement No. 777778 provided additional support. At Curtin University, The Institute for Geoscience Research (TIGeR) and by the Curtin Institute for Computation, kindly provide continuing support.

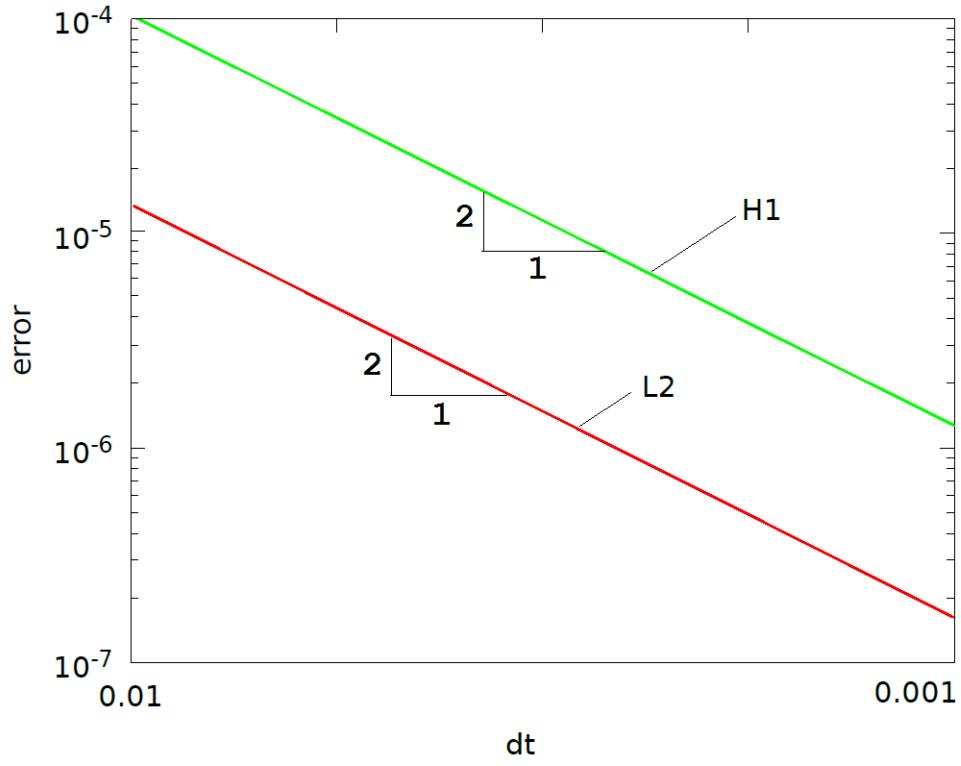


Figure 5: The second order time integration scheme for linear elasticity.

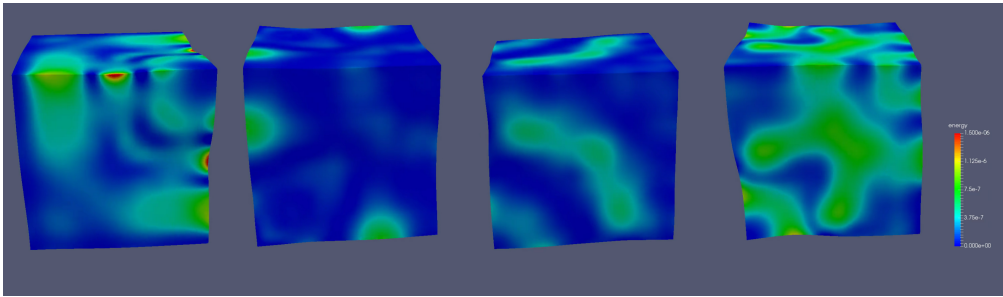


Figure 6: Stable simulation.

8. Appendix: Linear computational cost solver

The matrix $\mathcal{M} = \mathcal{M}^x \otimes \mathcal{M}^y$ has a Kronecker-product structure. Each of the matrices \mathcal{M}^ξ corresponds to the one-dimensional mass matrix in the direction ξ . In this case, we can factorize the problem with linear cost with respect to the total number of degrees of freedom in the system.

These one-dimensional matrices have entries that correspond to the integrals of the multiplication of the one-dimensional B-spline basis functions. These B-spline basis functions have local support over $p+1$ elements, so the one-dimensional matrices $\mathcal{M}^x, \mathcal{M}^y$ have a banded structure.

$$\mathcal{M}_{ij}^x = 0 \iff |i - j| > p \quad (54)$$

$$\begin{bmatrix} \mathcal{M}_{11}^x & \mathcal{M}_{12}^x & \mathcal{M}_{13}^x & \mathcal{M}_{14}^x & 0 & 0 & \cdots & 0 \\ \mathcal{M}_{21}^x & \mathcal{M}_{22}^x & \mathcal{M}_{23}^x & \mathcal{M}_{24}^x & \mathcal{M}_{25}^x & 0 & \cdots & 0 \\ \mathcal{M}_{31}^x & \mathcal{M}_{32}^x & \mathcal{M}_{33}^x & \mathcal{M}_{34}^x & \mathcal{M}_{35}^x & \mathcal{M}_{36}^x & \cdots & 0 \\ \vdots & \vdots & \vdots & \vdots & \vdots & \vdots & & \vdots \\ 0 & 0 & \cdots & \cdots & \mathcal{M}_{n(n-3)}^x & \mathcal{M}_{n(n-2)}^x & \mathcal{M}_{n(n-1)}^x & \mathcal{M}_{nn}^x \end{bmatrix}$$

where $\mathcal{M}_{ij}^x = (B_i^x, B_j^x)_{L^2}$. Same applies for \mathcal{M}_{ij}^y .

The Kronecker product structure of the matrix allows us to perform the following trick. Rather than solving a 3D problem, we can solve three one-dimensional problems with multiple right-hand-sides.

$$\begin{bmatrix} \mathcal{M}_{11}^x & \mathcal{M}_{12}^x & \mathcal{M}_{13}^x & \mathcal{M}_{14}^x & 0 & \cdots & 0 \\ \mathcal{M}_{21}^x & \mathcal{M}_{22}^x & \mathcal{M}_{23}^x & \mathcal{M}_{24}^x & \mathcal{M}_{25}^x & \cdots & 0 \\ \vdots & \vdots & \vdots & \vdots & \vdots & & \vdots \\ 0 & \cdots & 0 & \mathcal{M}_{n(n-3)}^x & \mathcal{M}_{n(n-2)}^x & \mathcal{M}_{n(n-1)}^x & \mathcal{M}_{nn}^x \end{bmatrix} \begin{bmatrix} x_{111} & x_{121} & \cdots & x_{1lm} \\ x_{211} & x_{221} & \cdots & x_{2lm} \\ \vdots & \vdots & \ddots & \vdots \\ x_{k11} & x_{k21} & \cdots & x_{klm} \end{bmatrix} = \begin{bmatrix} b_{111} & b_{121} & \cdots & b_{1lm} \\ b_{211} & b_{221} & \cdots & b_{2lm} \\ \vdots & \vdots & \ddots & \vdots \\ b_{k11} & b_{k21} & \cdots & b_{klm} \end{bmatrix}$$

$$\begin{bmatrix} \mathcal{M}_{11}^y & \mathcal{M}_{12}^y & \mathcal{M}_{13}^y & \mathcal{M}_{14}^y & 0 & \cdots & 0 \\ \mathcal{M}_{21}^y & \mathcal{M}_{22}^y & \mathcal{M}_{23}^y & \mathcal{M}_{24}^y & \mathcal{M}_{25}^y & \cdots & 0 \\ \vdots & \vdots & \vdots & \vdots & \vdots & & \vdots \\ 0 & \cdots & 0 & \mathcal{M}_{n(n-3)}^y & \mathcal{M}_{n(n-2)}^y & \mathcal{M}_{n(n-1)}^y & \mathcal{M}_{nn}^y \end{bmatrix} \begin{bmatrix} y_{111} & y_{211} & \cdots & y_{k1m} \\ y_{121} & y_{211} & \cdots & y_{k2m} \\ \vdots & \vdots & \ddots & \vdots \\ y_{1l1} & y_{1l1} & \cdots & y_{klm} \end{bmatrix} = \begin{bmatrix} x_{111} & x_{111} & \cdots & x_{k1m} \\ x_{121} & x_{211} & \cdots & x_{k2m} \\ \vdots & \vdots & \ddots & \vdots \\ x_{1l1} & x_{2l1} & \cdots & x_{klm} \end{bmatrix}$$

$$\begin{bmatrix} \mathcal{M}_{11}^z & \mathcal{M}_{12}^z & \mathcal{M}_{13}^z & \mathcal{M}_{14}^z & 0 & \cdots & 0 \\ \mathcal{M}_{21}^z & \mathcal{M}_{22}^z & \mathcal{M}_{23}^z & \mathcal{M}_{24}^z & \mathcal{M}_{25}^z & \cdots & 0 \\ \vdots & \vdots & \vdots & \vdots & \vdots & & \vdots \\ 0 & \cdots & 0 & \mathcal{M}_{n(n-3)}^z & \mathcal{M}_{n(n-2)}^z & \mathcal{M}_{n(n-1)}^z & \mathcal{M}_{nn}^z \end{bmatrix} \begin{bmatrix} z_{111} & z_{121} & \cdots & z_{1l1} \\ z_{212} & z_{222} & \cdots & z_{2l2} \\ \vdots & \vdots & \ddots & \vdots \\ z_{k1m} & z_{k2m} & \cdots & z_{klm} \end{bmatrix} = \begin{bmatrix} y_{111} & y_{121} & \cdots & y_{1l1} \\ y_{212} & y_{222} & \cdots & y_{kl2} \\ \vdots & \vdots & \ddots & \vdots \\ y_{k1m} & y_{k2m} & \cdots & y_{klm} \end{bmatrix}$$

where $\mathcal{M}_{ij}^x = (B_i^x, B_j^x)_{L^2}$ and $\mathcal{M}_{ij}^y = (B_i^y, B_j^y)_{L^2}$ and $\mathcal{M}_{ij}^z = (B_i^z, B_j^z)_{L^2}$. The dimensions of the first problem are $n \times n$, where n is the number of B-spline basis functions along x axis, and we have ml right-hand-sides, where m is the number of B-spline basis functions along y axis, and l is the number of B-spline basis functions along z axis. The computational complexity of factorization of such a system is $O(n * m * l) = O(N)$ [29]. We have the analogous situation in the second problem, namely $m \times m$ system with $n * l$ right-hand-sides, which results in $O(m * n * l) = O(N)$ linear computational complexity, and in the third system we have $l \times l$ system with $n * m$ right-hand-sides, which results in $O(l * n * m) = O(N)$ linear computational complexity.

This strategy delivers a solution to the isogeometric L2 projection problem with linear $O(N)$ computational cost. This solution method improves on the standard direct solver cost estimates for and $O(N^2)$ in three-dimensions, see [8]) for the factorization of the global problem.

References

- [1] Y. Bazilevs, L. Beirao da Veiga, J.A. Cottrell, T.J.R. Hughes, and G. Sangalli, *Isogeometric analysis: Approximation, stability and error estimates for h-refined*

- meshes*, Mathematical Methods and Models in Applied Sciences, 16 (2006) 1031–1090.
- [2] Y. Bazilevs, V.M. Calo, J.A. Cottrell, T.J.R. Hughes, A. Reali, G. Scovazzi, *Variational multiscale residual-based turbulence modeling for large eddy simulation of incompressible flows*, Computer Methods in Applied Mechanics and Engineering 197 (2007) 173-201.
 - [3] Y. Bazilevs, V.M. Calo, Y. Zhang, T.J.R. Hughes: *Isogeometric fluid-structure interaction analysis with applications to arterial blood flow*, Computational Mechanics 38 (2006).
 - [4] Y. Bazilevs, V. M. Calo, J. A. Cottrell, J. A. Evans, S. Lipton, M. A. Scott, T. W. Sederberg, *Isogeometric analysis using T-splines*, Computer Methods in Applied Mechanics and Engineering, 199 (2010) 229-263.
 - [5] G. Birkhoff, R.S. Varga, D. Young, Alternating direction implicit methods, Advanced Computing 3 (1962) 189-273.
 - [6] V.M. Calo, N. Brasher, Y. Bazilevs, T.J.R. Hughes, *Multiphysics Model for Blood Flow and Drug Transport with Application to Patient-Specific Coronary Artery Flow*, Computational Mechanics, 43(1) (2008) 161–177.
 - [7] K. Chang, T.J.R. Hughes, V.M. Calo, *Isogeometric variational multiscale large-eddy simulation of fully-developed turbulent flow over a wavy wall*, Computers and Fluids, 68 (2012) 94-104.
 - [8] N. Collier, D. Pardo, L. Dalcin, M. Paszyński, and V. Calo, The cost of continuity: A study of the performance of isogeometric finite elements using direct solvers, *Computer Methods in Applied Mechanics and Engineering*, (2012), 213, 353-361.
 - [9] J. A. Cottrell, T. J. R. Hughes, Y. Bazilevs, *Isogeometric Analysis: Toward Unification of CAD and FEA* John Wiley and Sons, (2009)
 - [10] L. Dedè, T.J.R. Hughes, S. Lipton, V.M. Calo, *Structural topology optimization with isogeometric analysis in a phase field approach*, USNCTAM2010, 16th US National Congress of Theoretical and Applied Mechanics.
 - [11] L. Dedè, M. J. Borden, T.J.R. Hughes, *Isogeometric analysis for topology optimization with a phase field model*, ICES REPORT 11-29, The Institute for

Computational Engineering and Sciences, The University of Texas at Austin (2011).

- [12] J. Douglas, H. Rachford, On the numerical solution of heat conduction problems in two and three space variables, Transactions of American Mathematical Society 82 (1956) 421-439.
- [13] R. Duddu, L. Lavier, T.J.R. Hughes, V.M. Calo, *A finite strain Eulerian formulation for compressible and nearly incompressible hyper-elasticity using high-order NURBS elements*, International Journal of Numerical Methods in Engineering, 89(6) (2012) 762-785.
- [14] L. Gao, V.M. Calo, Fast Isogeometric Solvers for Explicit Dynamics, Computer Methods in Applied Mechanics and Engineering, 274 (1) (2014) 19-41.
- [15] L. Gao, V.M. Calo, Preconditioners based on the alternating-direction-implicit algorithm for the 2D steady-state diffusion equation with orthotropic heterogeneous coefficients, 273 (1) (2015) 274-295.
- [16] L. Gao, Kronecker Products on Preconditioning, PhD. Thesis, King Abdullah University of Science and Technology (2013).
- [17] H. Gómez, V.M. Calo, Y. Bazilevs, T.J.R. Hughes, *Isogeometric analysis of the Cahn-Hilliard phase-field model*, Computer Methods in Applied Mechanics and Engineering 197 (2008) 4333-4352.
- [18] H. Gómez, T.J.R. Hughes, X. Nogueira, V.M. Calo, *Isogeometric analysis of the isothermal Navier-Stokes-Korteweg equations*. Computer Methods in Applied Mechanics and Engineering 199 (2010) 1828-1840.
- [19] J. L. Guermond, P. Mineev, *A new class of fractional step techniques for the incompressible Navier-Stokes equations using direction splitting*, Comptes Rendus Mathématique 348(9-10) (2010) 581-585.
- [20] J. L. Guermond, P. Mineev, J. Shen, *An overview of projection methods for incompressible flows*, Computer Methods in Applied Mechanics and Engineering, 195 (2006) 6011-6054.
- [21] G. Gurgul, M. Woźniak, M. Łoś, D. Szeliga, M. Paszyński, Open source JAVA implementation of the parallel multi-thread alternating direction isogeometric L2 projections solver for material science simulations, Computer Methods in Material Science (2017)

- [22] E. Hairer, G. Wanner, Solving ordinary differential equations II: Stiff and differential-algebraic problems (second ed.), Berlin: Springer-Verlag, section IV.3 (1996)
- [23] S. Hossain, S.F.A. Hossainy, Y. Bazilevs, V.M. Calo, T.J.R. Hughes, *Mathematical modeling of coupled drug and drug-encapsulated nanoparticle transport in patient-specific coronary artery walls*, Computational Mechanics, doi: 10.1007/s00466-011-0633-2, (2011).
- [24] M.-C. Hsu, I. Akkerman, Y. Bazilevs, *High-performance computing of wind turbine aerodynamics using isogeometric analysis*, Computers and Fluids, 49(1) (2011) 93-100.
- [25] M. Łoś, M. Woźniak, M. Paszyński, L. Dalcin, V.M. Calo, Dynamics with Matrices Possessing Kronecker Product Structure, Procedia Computer Science 51 (2015) 286-295
- [26] M. Łoś, M. Paszyński, A. Khusek, W. Dzwiniel, Application of fast isogeometric L2 projection solver for tumor growth simulations, Computer Methods in Applied Mechanics and Engineering, 316 (2017) 1257-1269.
- [27] M. Łoś, M. Woźniak, M. Paszyński, A. Lenharth, K. Pingali, IGA-ADS : Isogeometric Analysis FEM using ADS solver, Computer & Physics Communications, 217 (2017) 99-116.
- [28] N. M. Newmark, A method of computation for structural dynamics, Journal of Engineering Mechanics, ASCE, 85 (EM3) (1959) 67-94.]
- [29] M. Paszyński, Fast solvers for mesh-based computations, Taylor & Francis, CRC Press (2016)
- [30] D.W. Peaceman, H.H. Rachford Jr., The numerical solution of parabolic and elliptic differential equations, Journal of Society of Industrial and Applied Mathematics 3 (1955) 2841.
- [31] L. Piegl, and W. Tiller, *The NURBS Book (Second Edition)*, Springer-Verlag New York, Inc., (1997).
- [32] E.L. Wachspress, G. Habetler, An alternating-direction-implicit iteration technique, Journal of Society of Industrial and Applied Mathematics 8 (1960) 403-423.

- [33] M. Woźniak, M. Łoś, M. Paszyński, L. Dalcin, V. Calo, Parallel fast isogeometric solvers for explicit dynamics, *Computing and Informatics* 36(2) (2017) 423-448.
- [34] P. Behnoudfar, V. M. Calo, Q. Deng, P. D. Minev, A variationally separable splitting for the generalized- α method for parabolic equations, (2018) arXiv:1811.09351
- [35] G. Gurgul, M. Paszyński, Object-oriented implementation of the Alternating Directions Implicit Solver for Isogeometric Analysis, *Advances in Engineering Software* (2019) in press.
- [36] P. Behnoudfar, V. M. Calo, Q. Deng, P. D. Minev, A variationally separable splitting for the generalized- α method for parabolic equations. (2018) arXiv preprint arXiv:1811.09351 .
- [37] P. Behnoudfar, Q. Deng, V. M. Calo, V.M., Higher-order generalized- α methods for hyperbolic problems (2019) arXiv preprint arXiv:1906.06081 .
- [38] J. Chung, G. Hulbert, A time integration algorithm for structural dynamics with improved numerical dissipation: the generalized- α method. *Journal of Applied Mechanics* 60 (1993)
- [39] Q. Deng, P. Behnoudfar, V. M. V.M., High-order generalized- α methods (2019) arXiv preprint arXiv:1902.05253.
- [40] R. A. Horn, C. R. Johnson, *Matrix analysis*. Cambridge university press. (1990)
- [41] F. J. Lisbona, P. N. Vabishchevich, Operator-splitting schemes for solving unsteady elasticity problems. *Computational Methods in Applied Mathematics* 1 (1990) 188-198.
- [42] A. A. Samarskii, An economical algorithm for the numerical solution of systems of differential and algebraic equations. *USSR Computational Mathematics and Mathematical Physics* 4 (1964) 263-271.
- [43] Samarskii, A. A. and Matus, P. P. and Vabishchevich, P. N., Kluwer Academic Publisher, *Difference schemes with operator factors*, 2002,
- [44] R. A Horn, C. R. Johnson, *Matrix analysis*, 1990, Cambridge university press
- [45] P. Behnoudfar, V. M. Calo, Q. Deng, P. Minev, A variationally separable splitting for the generalized- α method for parabolic equations, arXiv preprint arXiv:1811.09351, 2018

- [46] K. E. Jennsen, C. Whiting, G. M. Hulbert, A generalized- α method for integrating the filtered Navier–Stokes equations with a stabilized finite element method, *Computer Methods in Applied Mechanics and Engineering*, 190, 3-4, 305–319, 2000, Elsevier
- [47] Q. Deng, P. Behnoudfar, V. M. Calo, High-order generalized- α methods, *arXiv preprint arXiv:1902.05253*, 2019
- [48] P. Behnoudfar, Q. Deng, V. M. Calo, Higher-order generalized- α methods for hyperbolic problems, *arXiv preprint arXiv:1906.06081*, 2019
- [49] M. Paszyński, L. Demkowicz, D. Pardo, Verification of goal-oriented HP-adaptivity, *Computers and Mathematics with Applications*, 50, 8-9, 2005, 1395-1404, Elsevier
- [50] M. Woźniak, M. Kuźnik, M. Paszyński, V. M. Calo, D. Pardo Computational cost estimates for parallel shared memory isogeometric multi-frontal solvers, *Computers and Mathematics with Applications*, 67, 10, 2014, 1864-1883, Elsevier